

## RESEARCH ARTICLE

10.1002/2016JA023359

## Key Points:

- Regional maps of TEC showing the existence of two regions of enhanced densities during two magnetic storms
- During the storms, the equatorial anomaly is weakly developed and does not contribute to the SED
- Neutral winds have an important role on producing TEC enhancements at midlatitudes during magnetic storms

## Supporting Information:

- Supporting Information S1
- Movie S1
- Movie S2

## Correspondence to:

C. E. Valladares,  
cev160230@utdallas.edu

## Citation:

Valladares, C. E., J. V. Eccles, S. Basu, R. W. Schunk, R. Sheehan, R. Pradipta, and J. M. Ruohoniemi (2017), The magnetic storms of 3–4 August 2010 and 5–6 August 2011: 1. Ground- and space-based observations, *J. Geophys. Res. Space Physics*, 122, 3487–3499, doi:10.1002/2016JA023359.

Received 18 AUG 2016

Accepted 3 JAN 2017

Accepted article online 7 JAN 2017

Published online 7 MAR 2017

## The magnetic storms of 3–4 August 2010 and 5–6 August 2011: 1. Ground- and space-based observations

C. E. Valladares<sup>1,2</sup> , J. V. Eccles<sup>3</sup>, Su. Basu<sup>1,4</sup>, R. W. Schunk<sup>3</sup> , R. Sheehan<sup>1</sup>, R. Pradipta<sup>1</sup> , and J. M. Ruohoniemi<sup>5</sup> 

<sup>1</sup>Institute for Scientific Research, Boston College, Newton, Massachusetts, USA, <sup>2</sup>Hanson Center for Space Sciences, University of Texas at Dallas, Richardson, Texas, USA, <sup>3</sup>Center for Atmospheric and Space Science, Utah State University, Logan, Utah, USA, <sup>4</sup>National Science Foundation, Arlington, Virginia, USA, <sup>5</sup>Bradley Department of Electrical and Computer Engineering, Virginia Tech, Blacksburg, Virginia, USA

**Abstract** We have used total electron content (TEC) values from low, middle, and high latitudes recorded over the American continent and density and ion temperature measured in situ by the DMSP-F15 and F17 satellites during the geomagnetic storms of 3–4 August 2010 and 5–6 August 2011 to study the formation and dynamics of plasma density enhancements that developed during these two storms. Common to both storms are the timing of the main phase that extends between 20 and 24 UT and their seasonality with both storms occurring near the end of the Northern Hemisphere summer solstice. During both storms, TEC data show incipient equatorial anomalies lacking a poleward expansion beyond 20° magnetic latitude. Two large-scale TEC enhancements were observed at middle latitudes showing a complicated pattern of structuring and merging. The first TEC enhancement corresponds to a storm-enhanced density (SED) seen between 21 and 01 UT on the following day. The second TEC enhancement was observed over Central America, located equatorward of the SED and apparently moving northward. However, careful analysis of the TEC values indicates that this second TEC enhancement is not transported from lower latitudes through a superfountain effect. Instead, the enhanced plasma has a local origin and is driven by a southward directed meridional wind that moves plasma up the tilted magnetic field lines. DMSP flights passing over the second TEC enhancement show a reduction of the ion temperature, confirming an adiabatic expansion of the plasma as it moves up the field lines. It is concluded that the midlatitude TEC enhancements do not arise from a low-latitude ionospheric fountain effect.

### 1. Introduction

This series of two papers present the results of an investigation of the physical mechanisms responsible for the initiation and evolution of two large-scale total electron content (TEC) enhanced structures seen in the American sector during the magnetic storms of 3–4 August 2010 and 5–6 August 2011. In this paper, we present detailed ground- and space-based observations of the large-scale TEC enhancements that developed during both magnetic storms. The modeling and simulations have been described in a companion paper (J. V. Eccles et al., The magnetic storms of August 3–4, 2010 and August 5–6, 2011: 2. Ionosphere and electrodynamics modeling, in preparation, 2017). The first TEC enhancement was initially seen over the eastern part of North America, corresponding to a growing storm-enhanced density (SED). This enhancement was centered at 40°N, 83°W at 22:20 UT on 3 August 2010. The second TEC enhancement was initially located over Central America and comprised a large-scale region that expanded parallel to and equatorward of the SED. The second TEC enhancement has a center at 18°N, 97°W.

SEDs are persistent ionospheric features observed in the pre-midnight subauroral ionosphere during the main phase of magnetic storms [Foster, 1993; Foster and Rich, 1998]. Global maps of TEC have revealed that SEDs are wedge-type structures containing enhanced plasma that move poleward toward the cusp. The Millstone Hill incoherent scatter radar has been instrumental in characterizing SEDs as spatially continuous, large-scale features spanning local times between noon and midnight and extending between the trough and the midlatitude ionosphere [Foster et al., 2005].

Several different theories have been presented to explain the origin of the high-density plasma that is found within the SEDs. Vlasov et al. [2003] were the first to use a theoretical model to suggest that the prompt penetration of a strong electric field to middle and low latitudes was able to produce the high

TEC enhancements at the crests of the equatorial anomaly and then displace the crests farther poleward to reach higher latitudes. Later, *Kelley et al.* [2004] suggested that the crest density itself could be driven poleward by a penetrating zonal electric field to form SEDs. A comprehensive set of measurements was presented by *Tsurutani et al.* [2004] in which satellite and ground GPS data were used to demonstrate that the entire low and middle latitudes (up to  $\pm 50^\circ$ ) ionospheres were uplifted during the storm of 5–6 November 2001. These authors concluded that the pronounced uplift was the result of a dayside latitudinally extended superfountain effect able to transport equatorial plasma upward and reach midlatitudes by diffusion along the field lines [*Mannucci et al.*, 2005]. It was also pointed out that the rapid uplift of the ionosphere could also set off plasma instabilities to form bubbles and depletions [*Basu et al.*, 2007]. *Balan et al.* [2009] used the Sheffield University Plasmasphere-Ionosphere Model to demonstrate that an equatorward wind can produce stronger crests of the equatorial anomaly by reducing the downward diffusion of plasma along the field lines associated with the superfountain effect.

These initial hypotheses were followed by more comprehensive measurements and modeling work. *Heelis et al.* [2009] used the Time-Dependent Ionospheric Model [*Schunk et al.*, 1986; *Schunk*, 1988; *Sojka*, 1989] to demonstrate that an expanded auroral oval, as commonly occurs during magnetic storms [*Heelis and Mohapatra*, 2009], was sufficient to create dayside SED-type TEC enhancements amplified by a factor of 2 or more. Hence, there was not a requirement for the plasma to be first enhanced in the equatorial ionization anomaly and then transported to midlatitudes. In addition, *Rishbeth et al.* [2010] questioned the ability of a density enhancement to withstand the long transport times required for the “superfountain effect” plasma to reach high latitudes. They also pointed out that this time, several hours, is much longer than the lifetime of the plasma even at high altitudes. *Tsurutani et al.* [2013] responded that the effect of the variability of the prompt penetration electric field and disturbance neutral wind should be considered in a very complete modeling of the low-, middle-, and high-latitude ionosphere. It is worth mentioning that *Vlasov et al.* [2003] suggested that a daytime southward neutral wind could produce a TEC enhancement by moving plasma toward higher altitudes of reduced chemical loss. This effect would be the largest near  $\pm 30$  magnetic latitude [*Balan et al.*, 2010].

It is presently known that several processes in the coupled magnetosphere-ionosphere-thermosphere system can induce intense changes in the regional and global distribution of plasma densities. These changes are more pronounced during disturbed conditions in which *F* region densities can increase, or decrease, by a factor of 5–10. Penetration electric fields can lead to increases in the ionospheric density by raising the layer height; they modify the fountain effect at the equator and transport the crests of the equatorial anomaly poleward [*Mannucci et al.*, 2005]. Thermospheric heating at the poles produces a southward wind pattern, driving the ionospheric plasma up the field lines. Heating can also generate changes in the neutral composition. An increase in the molecular components in the *F* region can create an increase in the recombination rate and so reduce plasma density [*Crowley et al.*, 2006]. It is also pointed out that plasma instabilities can also create pronounced redistributions of the midlatitude plasma by the generation of medium-scale traveling ionospheric disturbances [*Perkins*, 1973]. It is the purpose of this paper to provide a thorough description of the ionospheric observations during two magnetic storms that developed during the ascending phase of solar cycle 24. During the last few years the number of GPS receivers operating in South and Central America and the Caribbean region has increased considerably allowing us to have the needed spatial resolution to understand the dynamics of several large-scale ionospheric processes. One of these networks belongs to the low-latitude ionospheric sensor network (LISN) [*Valladares and Chau*, 2012]. This paper presents ground- and space-based observations obtained during the storm of 3–4 August 2010 (section 2) and the storm of 5–6 August 2011 (section 3). The paper concludes with a discussion (section 4) and a list of the conclusions (section 5).

## 2. Observations During the Magnetic Storm of 3–4 August 2010

### 2.1. Solar Wind Parameters

On 3 August 2010 a moderate storm (G2 level) impinged on the magnetosphere at 1740 UT and lasted for nearly 12 h. The storm solar inputs can be seen in Figure 1, where we show the *SYM-H* parameter, the solar wind velocity, the proton density, and the  $B_z$  and  $B_y$  components of the interplanetary magnetic field (IMF) measured by the ACE satellite. Figure 1 (first panel) displays a positive increase in *SYM-H* to 30 nT that points to a compression of the magnetosphere under northward conditions. At the time of the shock, the solar wind

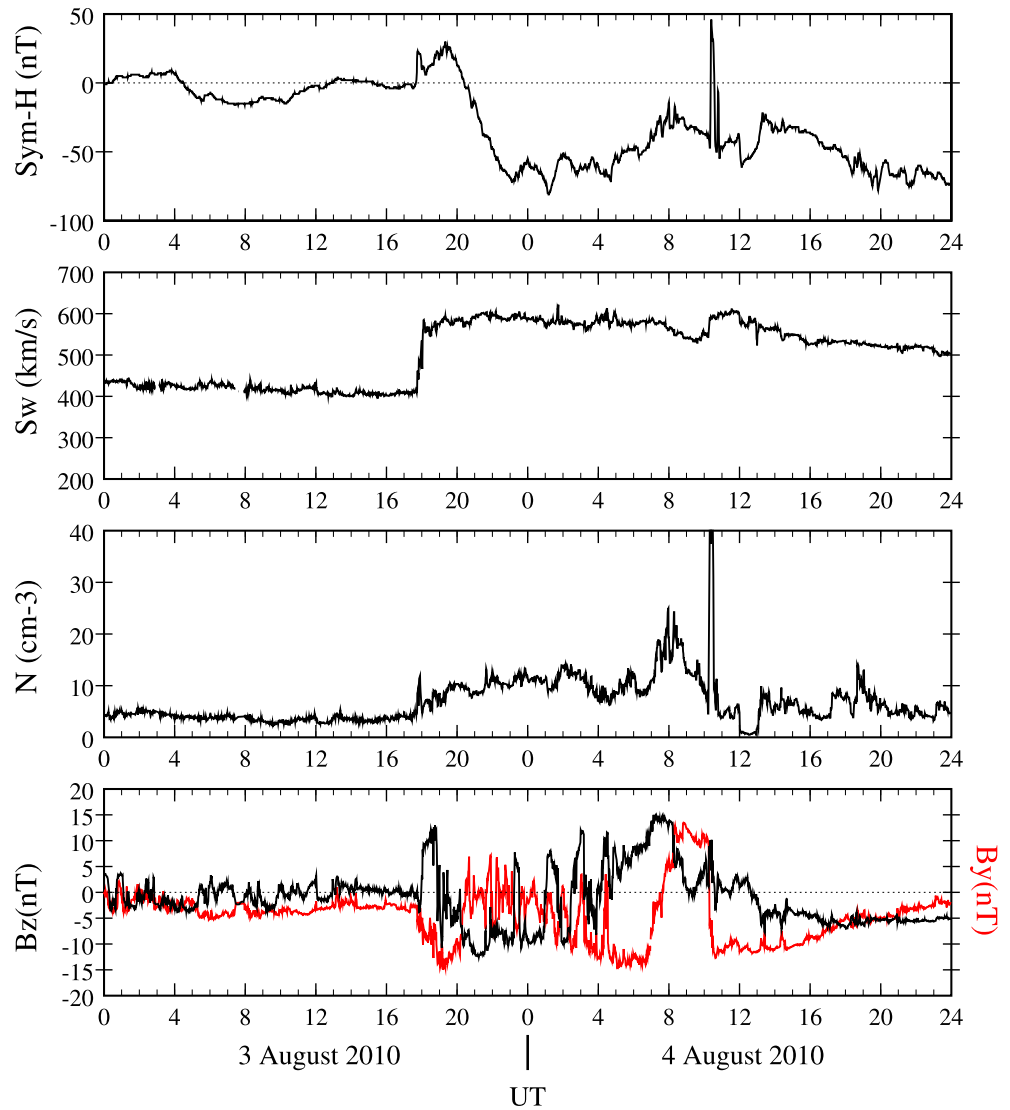


**Figure 1.** *SYM-H* index and interplanetary data corresponding to the storm event of 3–4 August 2010. The interplanetary data were measured by the ACE satellite. From top to bottom, the four frames show the 1 min *SYM-H* index (nT), the solar wind velocity (km/s), the solar wind proton density ( $\text{cm}^{-3}$ ), and the IMF  $B_z$  and  $B_y$  components (nT) displayed in black and red.

velocity suddenly rises to 600 km/s; however, the proton density increases slowly from 4 to 10 protons/ $\text{cm}^3$  between 1800 and 0100 UT on the following day. *SYM-H* starts decreasing at 1920 UT due to the southward turning of the IMF  $B_z$  component that occurs at  $\sim$ 1900 UT. This is followed by a series of  $B_z$  sign fluctuations that last until 1930 UT when a sustained period of strong southward IMF ( $-13$  nT) starts and last for 5 h. The IMF  $B_y$  component is negative between the time of the shock and the start of the main phase. The storm main phase starts at 1930 UT and lasts until 0100 UT on 4 August 2010 when  $B_z$  turns northward for a 40 min period. During the storm main phase,  $B_y$  presents continuous 15 min fluctuations that last until 2400 UT.

**2.2. TEC Values During the Magnetic Storm**

We processed RINEX files from 562 GPS stations that were operating in North, Central, and South America and the Caribbean region on 3–4 August 2010 to study TEC variability produced by this storm in the high-, middle-, and low-latitude ionospheres. The GPS receivers belong to several networks that are presently operating in the American sector. Some of these networks are global such as Continuously Operating Reference Stations, others are regional such as LISN, University NAVSTAR Consortium, and Sistema de Referencia Geocéntrico para las

Américas (SIRGAS). A total of 260 stations from North America and 300+ stations from South and Central America and the Caribbean region were utilized to produce the TEC maps in Figure 2.

The analysis of the RINEX files to derive equivalent vertical TEC values has been described in a previous publication [Valladares and Chau, 2012]. The algorithm that is used to interpolate and produce the regional TEC images has also been described before. Succinctly, this method consists of dividing the continent into thousands of overlapping areas that extend  $8^\circ$  in longitude and  $8^\circ$  in latitude. A 10-term, 2-D, third-order polynomial that varies as a function of latitude and longitude is least squares fitted to all TEC values in this square to find only four TEC values at the center of each overlapping square in a small area that is only  $1^\circ$  on each side. A new  $8^\circ \times 8^\circ$  area is considered by successively advancing  $1^\circ$  in latitude and then  $1^\circ$  in longitude. Commonly, a total of 15,000 fitted values are obtained per image.

The four images in Figure 2 illustrate the high spatial variability of the TEC values during the magnetic storm of 3–4 August 2010. Movie S1 in the supporting information consisting of 2 min frames and spanning between 2000 and 0300 UT is used to display the high temporal variability of the TEC images. The movie is part of the supporting information that accompanies this publication. Figure 2 shows still TEC images for (a) 2130 UT, (b) 2220 UT, (c) 2310 UT, and (d) 0100 UT. Satellite trajectories corresponding to two consecutive passes of the DMSP-F15 satellite across the American sector are indicated using a red line in Figures 2a and 2c. During the early part of the storm, the low-latitude ionosphere displays a weak equatorial anomaly containing a latitudinal extension not larger than  $5^\circ$  (Figure 2a). Only the southern crest is observed at this time. The anomaly starts expanding poleward near 2200 UT, reaches  $15^\circ$  magnetic latitude and becomes relatively more intense at 0100 UT. The northern crest does not appear until 2310 UT (Figure 2c) when it seems to be part of a region containing much higher TEC values located north of the anomaly (Figures 2a–2d). These high TEC values, named here the second TEC enhancement, could be mistaken for the crests of an anomaly that has expanded poleward to more than  $20^\circ$  in magnetic latitude driven by a superfountain effect. Instead, these high TEC values, as we show later, have a local origin.

The SED starts forming at 2020 UT (1520 LT at  $75^\circ\text{W}$ ), when it is seen as a faint enhancement located north of  $50^\circ$  geographic latitude. At 2050 UT, the SED appears as a narrow continuous line that enters the North American continent at  $42^\circ$  geographic latitude and leaves through Northern Canada at  $145^\circ\text{W}$  when it is directed into the cusp region forming the tongue of ionization (TOI). The SED as a whole starts moving southward at 2200 UT and continues to move southward for more than  $10^\circ$  in latitude between 2100 and 0100 UT. The eastern side of the SED widens over the eastern coast of North America and becomes aligned in the northwest-southeast direction at 0020 UT (1920 LT at  $75^\circ\text{W}$ ) on 4 August 2010. A close inspection of the TEC images show the SED developing undulations, as seen in its poleward boundary between  $110$  and  $100^\circ\text{W}$ , in Figures 2b and 2c. The TEC movie for 3–4 August 2010 indicates that a large segment of the SED intensifies slowly but concurrently between 2100 and 0100 UT. It also shows the northern end of the SED entering the polar cap through northern Alaska and becoming a narrow TOI at 2300 UT ( $\sim 13$  LT). The SED persists until 0100 UT, when it diminishes and fades. Near 0010 UT on 4 August 2010 a long and wide trough forms and extends parallel and poleward of the SED. The trough stays until 0400 UT, well within the recovery phase of the storm.

The second TEC enhancement becomes visible in the TEC maps before 2000 UT (14 LT at  $90^\circ\text{W}$ ) and seems to be part of a TEC enhanced feature that develops almost every day over the Central America-Mexico region during the June solstice season. However, on the day of the storm, the second TEC enhancement occupies a much larger area and lasts for many more hours. Figure 2a shows the second TEC enhancement located above Central America extending as far south as the northern boundary of Peru and to the north bounded by the central part of Mexico. A careful inspection of the movie for 3–4 August 2010 indicates that the second TEC enhancement weakens and becomes narrower at 2140 UT, when a resurgence of this enhancement occurs and last until 0030 UT of 4 August 2010, when there is a general decrease of all TEC structures. It is important to note that most of these observations correspond to local daytime hours when solar radiation is able to replenish bottomside plasma that may have moved up to higher altitudes. As night progresses, the second TEC enhancement grows northward and eastward reaching the middle part of the USA and merging with the southern boundary of the SED where it develops a system of fingers that seems to connect both regions of enhanced TEC values. Both regions of enhanced TEC seem to be fully merged at 2300 UT (17 LT at  $90^\circ\text{W}$ ), but they decay and separate at 2356 UT. After the start of day 4 August 2010, the northern part of the SED and the second enhancement decay very rapidly, and only their southern parts over the Central American and the Caribbean region remain, starting to fade by 0100 UT.

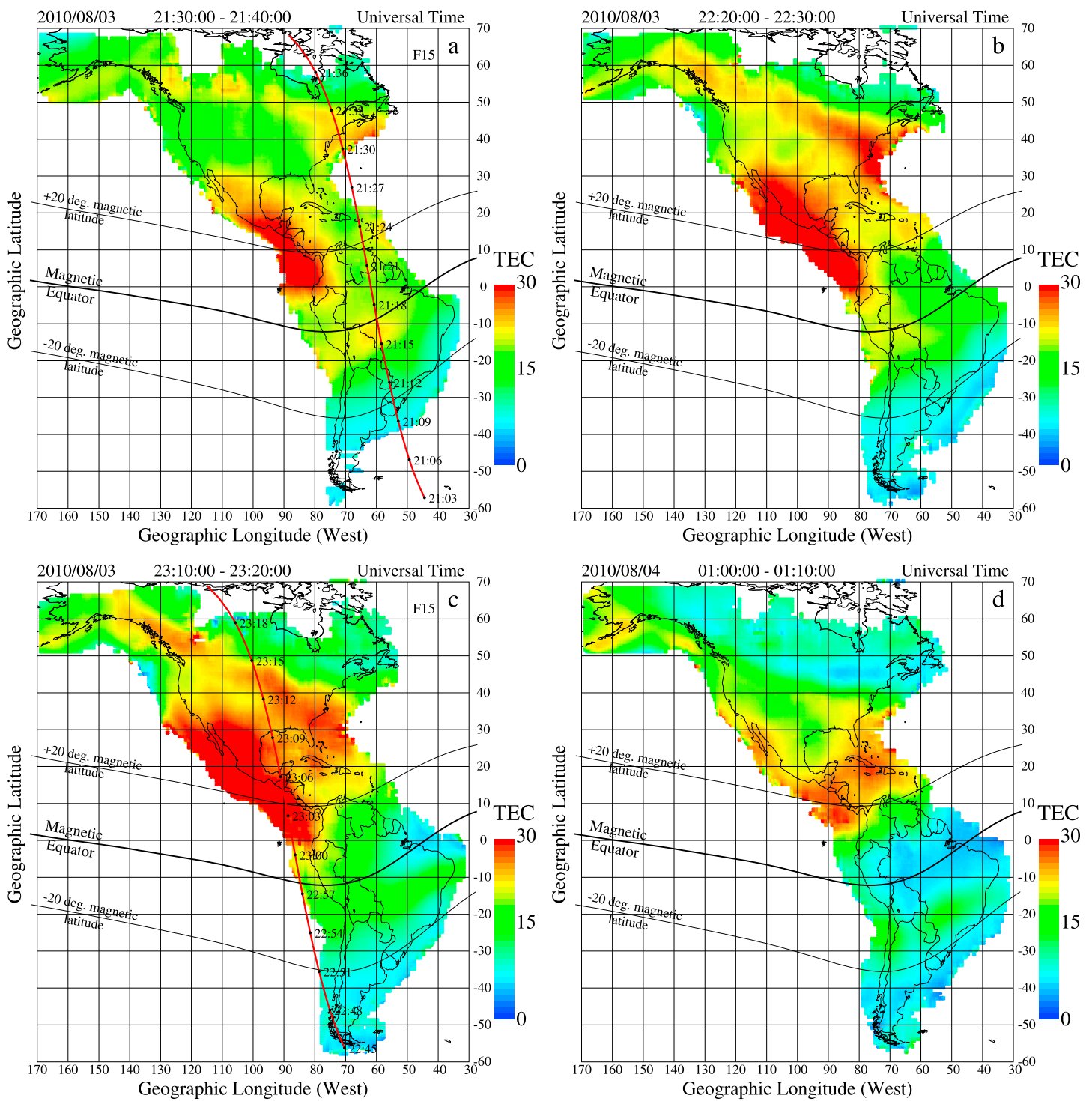


**Figure 2.** Total electron content measured by the LISN and several networks of GPS receivers that operate in North, Central and South America, and the Caribbean region. The four frames correspond to the following times: (a) 21:30–21:40 UT, (b) 22:20–22:30 UT, (c) 23:10–23:20 UT, and (d) 01:00–01:10 UT. Figures 2a and 2c show the trajectory of two consecutive passes of DMSP-F15.

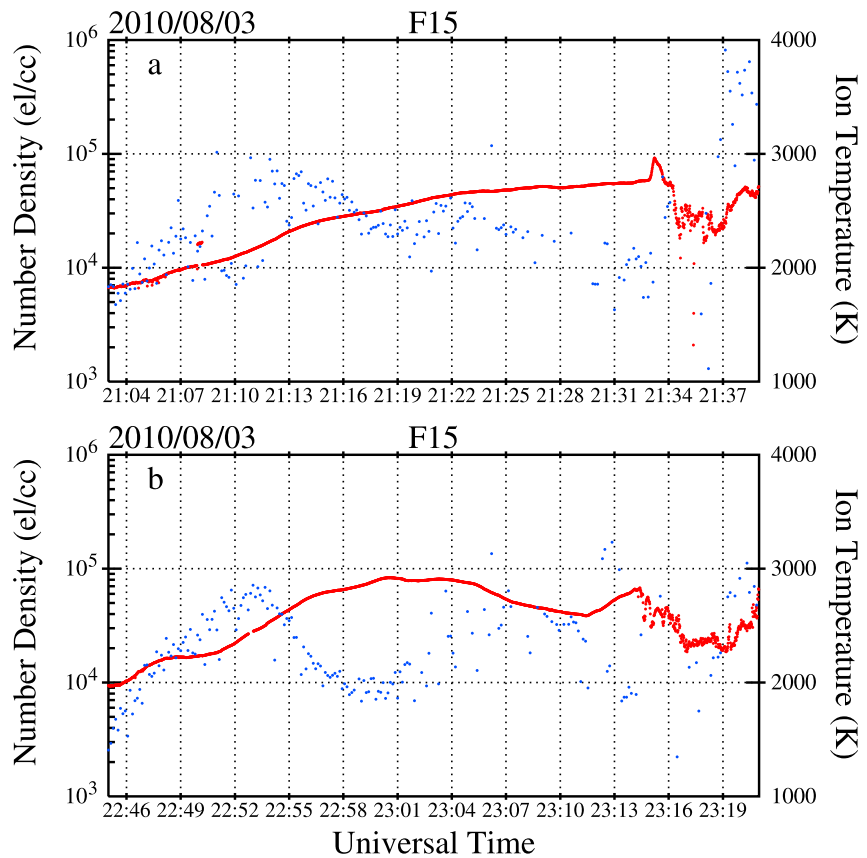


**Figure 3.** (a) The number density displayed as a red line and the ion temperature (blue dots) measured by the DMSP-F15 between 21:03 and 21:30 on 3 August 2010. (b) The same parameters measured by DMSP-F15 in the consecutive orbit between 22:45 and 23:23:21 UT.

### 2.3. DMSP In Situ Observations During the Storm

Figure 3 shows in situ number density (red trace) and ion temperature (blue dots) measured by the DMSP-F15 satellite orbiting at 840 km altitude between (a) 2104 and 2137 UT and (b) 2246 and 2319 UT. DMSP-F15 flies in circular, Sun-synchronous, polar orbit near the 2100–0900 local time meridian. Both density and ion temperature were measured by the Special Sensor for Ions, Electrons and Scintillations (SSIES) instrument. The purpose of these plots is to ascertain whether or not a link exists between the TEC enhancements observed by the GPS receivers, corresponding density enhancements at the satellite altitude, and low ion temperatures due to adiabatic cooling that may be produced by plasma moving up the field lines. Figure 3a shows a small density enhancement that is located equatorward of the trough at 2133 UT. This small  $N_e$  enhancement coincides with the poleward edge of the SED observed in Figure 2a. The second DMSP-F15 pass (Figure 3b) intersected both the SED and the second TEC enhancement. Two density enhancements are seen in Figure 3b corresponding to both TEC maxima observed in Figure 2c. However, a close comparison of the times and locations of both sets of enhancements indicates that there exists an apparent offset between TEC and density enhancements. The TEC enhancements detected with the GPS receivers appear to be located a few degrees north of the density increases detected in situ by the DMSP-F15 satellite. This discrepancy is more evident during the crossing of the second TEC enhancement in which the density increase was seen between 2259 and 2305 UT (Figure 3b), and the TEC enhancement crossing occurs between 2301 and 2307 UT along the satellite trajectory (see Figure 2c). This difference can be explained by the intrinsic characteristics of the measurements. GPS TEC is an altitude-integrated measurement that responds directly to the peak of the density profile, which is assumed to be at 350 km altitude. DMSP observations with the SSIES instrument are carried out at 840 km altitude. We suggest that after the *F* region plasma is set in motion, due to winds along the field lines, the plasma continues to move along the field lines and reaches 840 km altitude a few degrees farther to the south. As the TEC enhancements

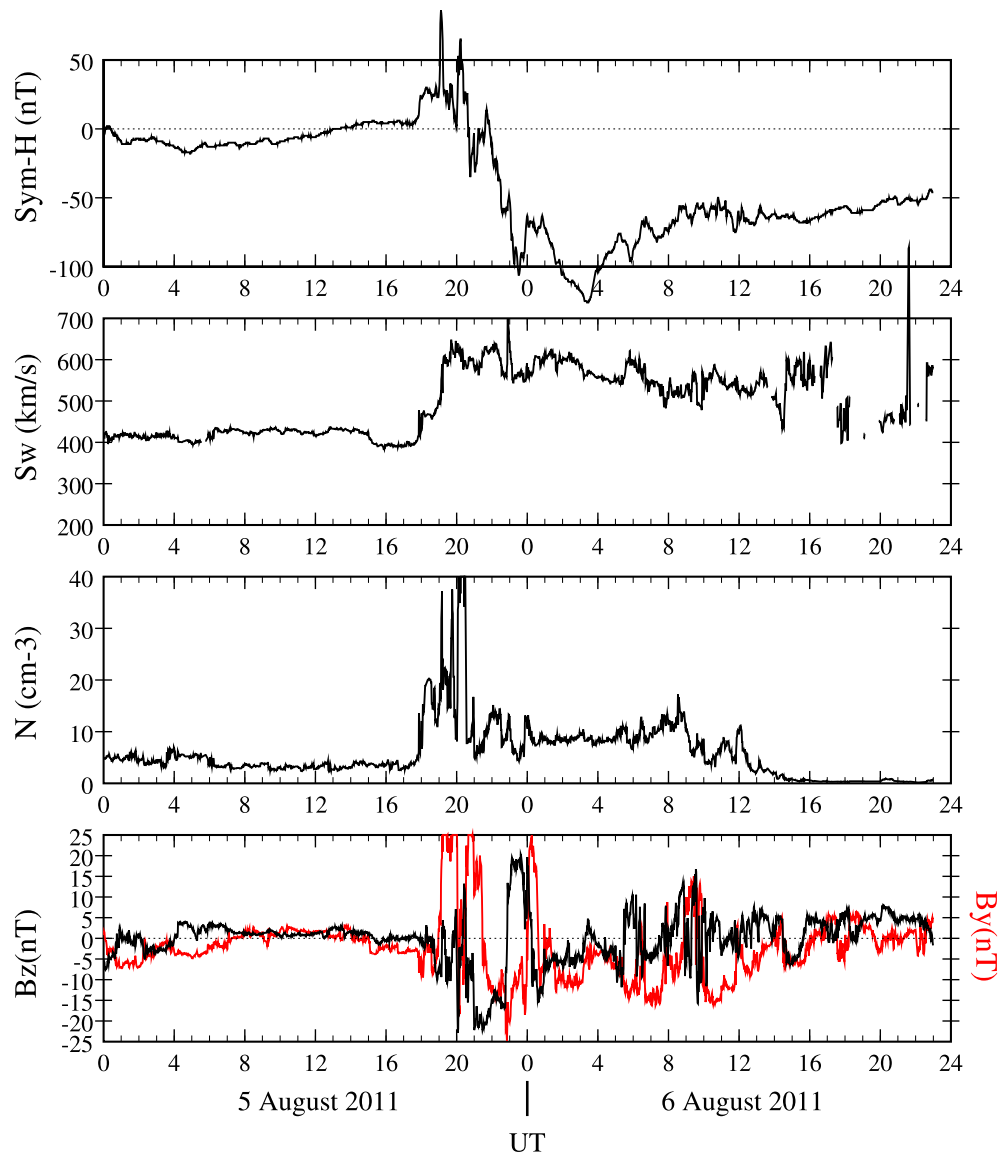


Figure 4. Same as Figure 1 but corresponding to 5–6 August 2011.

occur closer to the magnetic equator, where the inclination of the field line is smaller, a larger discrepancy is expected. It is also noted that  $T_i$  becomes less than 2000 K between 2258 and 2301 UT when DMSP-F15 is crossing the second TEC enhancement, giving credence to the hypothesis that this enhancement is due to a meridional neutral wind that moves the plasma up the field lines and into regions of smaller recombination rates.

### 3. Observations During the Magnetic Storm of 5–6 August 2011

#### 3.1. Solar Wind Parameters

A moderate magnetic storm developed on 5–6 August 2011 due to a sudden increase in the solar wind velocity from 400 to more than 600 km/s that occurred between 1800 and 1900 UT. On this day, the solar wind density increased rapidly reaching 20 proton/cm<sup>3</sup> before 1830 UT. The main phase of the storm started near 2000 UT, as indicated in Figure 4 by the sharp decrease in the SYM-H index. The SYM-H index diminished and reached –126 nT at 0322 UT on 6 August 2011 when a slow recovery phase was initiated and continued for several days. The SYM-H index did not return to the prestorm near-zero values until 13 August 2011. The

IMF  $B_z$  component was negative at the time of the storm commencement but exhibited a series of sign reversals that last until 2035 UT when a sharp decrease made  $B_z$  equal to  $-20$  nT. The IMF  $B_z$  component remained negative until  $\sim 0330$  UT except for a sharp positive excursion between 2300 and 0020 UT on 6 August 2011. We chose to study this storm and the one on 3–4 August 2010 due to their similarity on the main phase UT and the timing of the  $B_z$  southward reversals. It was indicated before that  $B_z$  became negative  $\sim 1930$  UT on 3 August 2010 and at 2035 UT on 5 August 2011.

### 3.2. TEC Values During the Storm of 5–6 August 2011

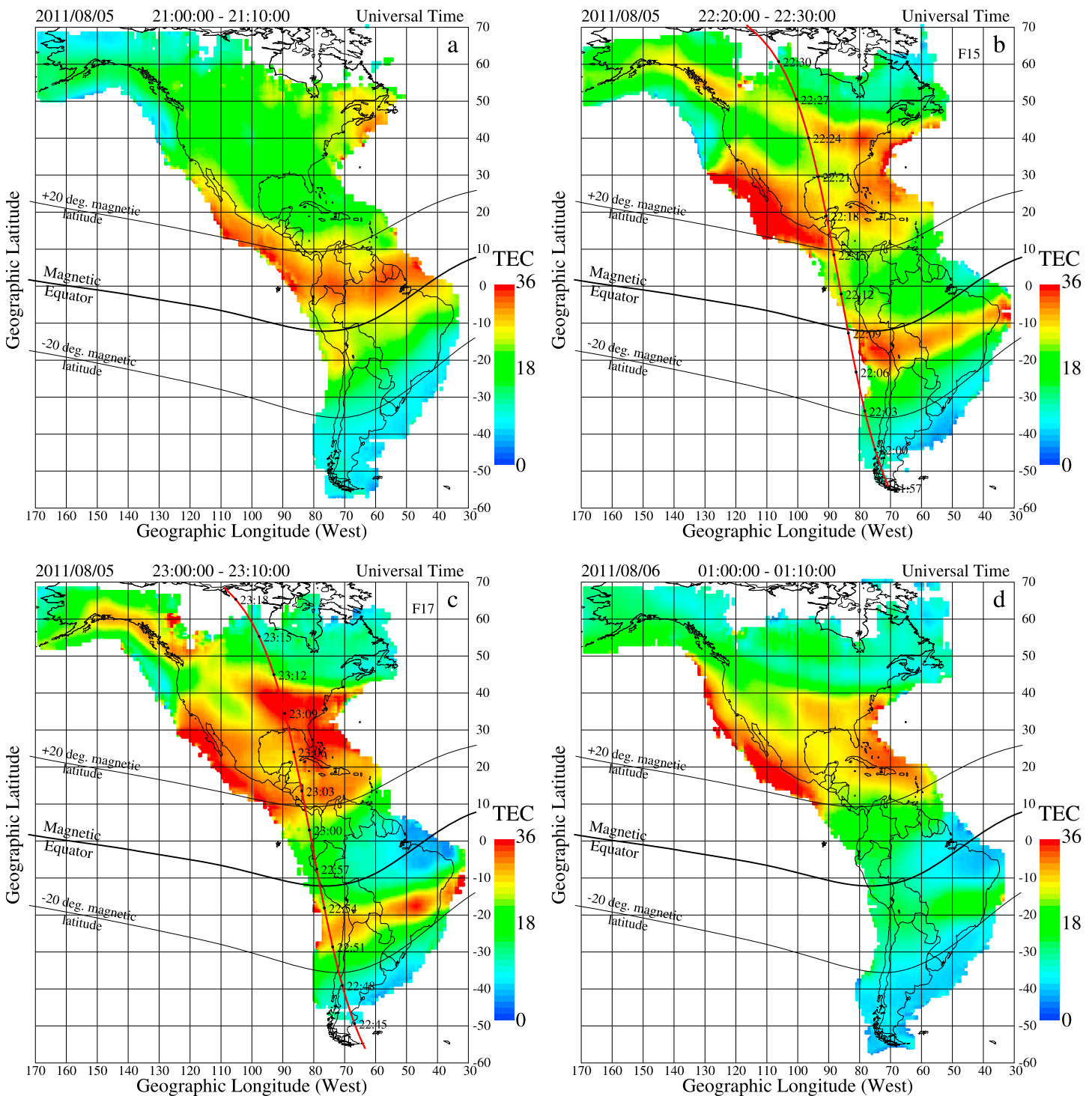
Equivalent vertical TEC values observed with 652 GPS receivers that operated continuously in the American sector were used to produce TEC maps during the storm of 5–6 August 2011 (Figure 5). We selected a variable time interval between the four frames of Figure 5 to accommodate a display of the DMSP-F15 satellite trajectory that crossed the American sector between 2157 and 2230 UT and the DMSP-F17 satellite trajectory between 2245 and 2318 UT. We will use these plots to ease the comparison between TEC and satellite Ne and Ti measurements. TEC images with a cadence time of 2 min were also processed to produce a movie that is included in the supporting information (Movie S2). Careful examination of the four frames of Figure 5, and an inspection of the movie, indicates the existence of an equatorial anomaly consisting of a single crest that is initially located in the Northern Hemisphere and later drifts to the Southern Hemisphere. The TEC movie starts at 1900 UT when the maximum TEC associated with the anomaly resides over the magnetic equator in the Brazilian sector. As time progresses, a single crest anomaly becomes fully formed that expands northward reaching  $+15^\circ$  magnetic latitude at 2130 UT (1630 LT at  $75^\circ$ W). After this time the anomaly recedes, fades a little and crosses the magnetic equator at 2205 UT. In the Southern Hemisphere, the crest reintensifies, expands poleward (Figure 5b), and develops a strong longitudinal variability in which the western side (Peruvian sector) is only  $10^\circ$  from the magnetic equator, but the eastern side (Brazilian sector) is situated at  $20^\circ$  magnetic latitude (Figure 5c). We believe that the poleward expansion and the reintensifications of the crest are likely produced by the action of the zonal electric fields related to a prompt penetration  $E$  field and an enhanced meridional neutral wind associated with storm conditions.

Similar to the TEC observations during the storm discussed in section 2, the TEC plots for 5–6 August 2011 show two TEC enhancements: (1) over North America and (2) along Central America. These two enhancements reach values higher than the TEC values of the equatorial anomaly. The SED appears initially over the eastern coast of North America ( $\sim 50^\circ$  geographic latitude) but rapidly expands westward by 2020 UT. Previous to the appearance of the SED, we did not observe low-latitude plasma density moving toward the region of the SED. In fact, the equatorial anomaly was moving farther southward away from the SED. During the following tens of minutes, the SED intensifies, drifts southward, and widens. The largest width is observed on the eastern side of the SED, where the enhanced plasma extends into the Caribbean region. Figures 5b and 5c, and the movie for 5–6 August 2011, display the growth and expansion of the SED into the Caribbean region occurring between 2200 and 2300 UT. This enhancement reaches the northern boundary of South America near 2300 UT (1800 LT at  $75^\circ$ W).

The second TEC enhancement appears at 1920 UT, tens of minutes before the start of the main phase, when a region of high TEC appears to move from the Pacific Ocean toward Central America. This enhancement expands over Mexico and the southern states on the west coast of USA between 2000 and 2130 UT. Similar to the enhancements observed on 3–4 August 2010, both TEC enhancements of 5–6 August 2011 merge (Figure 5c), coalesce, and then fade after 0200 UT. However, the final fate of both merged TEC enhancements includes a final splitting and a fading stage in which one enhancement decays and retreats over Central America and the southern part of the SED drifts over Florida and covers part of the Caribbean region. The TEC trough forms after 2300 UT and becomes very pronounced at 0100 UT (Figure 5d).

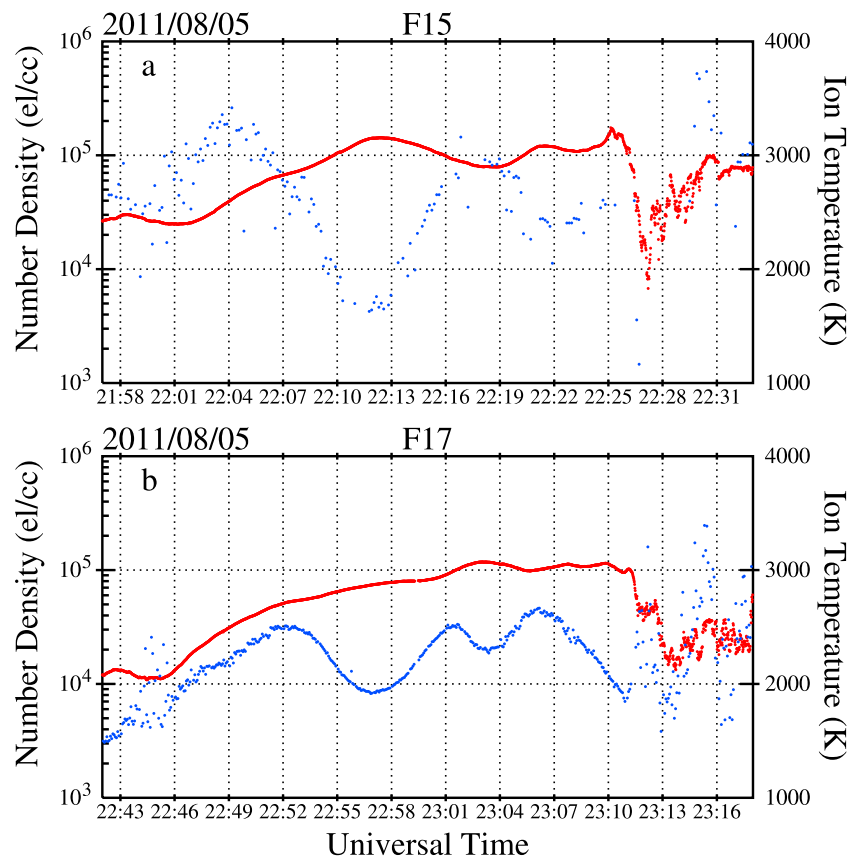
### 3.3. DMSP In Situ Observations During the Storm of 5–6 August 2011

Figure 6 shows the number density (in red) and the ion temperature (in blue) measured by the DMSP-F15 satellite between 2158 UT and 2231 UT and DMSP-F17 between 2243 and 2316 UT. The format of this Figure is similar to Figure 3, but during this storm a much higher variability was observed in both density and  $T_i$  parameters. A close comparison of the satellite trajectories (Figures 5b), the TEC values, and the Ne values of Figure 6a indicates that the small density peak seen at 2225 UT coincides with the TEC SED located between  $40^\circ$  and  $46^\circ$  geographic latitude at  $97^\circ$ W geographic longitude that was traversed by the DMSP-F15



**Figure 5.** Same as Figure 2 but corresponding to 5–6 August 2011. GPS TEC maps for (a) 21:00–21:10, (b) 22:20–22:30, (c) 23:00–23:10, and (d) 01:00–01:10 UT. Figures 5b and 5c show passes of the DMSP-F15 and F17, respectively.

satellite between 2224 and 2226 UT. The second density maxima observed by DMSP-F15 at 2212 UT is located few degrees south from the second TEC enhancement. It is worth mentioning that the density peak is associated with a significant decrease of the ion temperature to a value close to 1700 K. It is suggested that the ion temperature decrease is likely produced by adiabatic cooling due to the upward expansion of the F region



**Figure 6.** Same as Figure 3 but corresponding to 5–6 August 2011.

plasma carried by a southward directed wind. The spatial offset between the ground-based TEC and the satellite-observed density is due to the altitude difference between the two types of measurement.

Figure 6b displays density variations that are accompanied by pronounced changes in the ion temperature. A small density variability occurs during the satellite crossing of the SED. Here  $T_i$  decreases to values less than 2000 K at 2311 UT. A second, but smaller,  $T_i$  decrease was observed between 2302 and 2306 UT that occurred simultaneously with a small density increase observed when the DMSP-F17 satellite was crossing the second TEC enhancement and the southern part of the SED. This pattern of high Ne and low  $T_i$  supports our contention by which the formation of the second TEC enhancement is driven by a southward directed meridional wind that moves plasma along field lines toward higher altitudes where recombination proceeds at a slower rate. Both satellite passes of Figure 6 detected a prominent trough located adjacent to, but poleward of, the SED. The topside plasma density decreased by almost an order of magnitude to values close to  $10^4 \text{ cm}^{-3}$ . However, TEC decreases in the trough region are not observed in the TEC maps until 0100 UT on 6 August 2011 (Figure 5d and Movie S2). This fact suggests that plasma evacuation in the trough region starts in the topside ionosphere and later propagates and extends through all altitudes.

#### 4. Discussion

This paper has shown how the TEC evolved in the American sector during two magnetic storms that occurred during the ascending phase of the Sun's activity in cycle 24. The *SYM-H* index decreased to values close to  $-90 \text{ nT}$  and  $-120 \text{ nT}$  during the storms of August 2010 and 2011, respectively. These values are less negative than the *SYM-H* values observed during several superstorms that developed during solar cycle 23 [Basu et al., 2001, 2007; Vlasov et al., 2003; Tsurutani et al., 2004; Mannucci et al., 2005; Foster and Coster, 2007; Balan et al., 2009]. Here the effects of these two storms are thoroughly investigated, and each ionospheric process is singled out to investigate how they produce regions of enhanced densities (and TEC). It is also indicated that these processes can be magnified during super geomagnetic storms.

One of the processes, which has been cited as a way to redistribute plasma across latitudinal boundaries and produce density enhancements during magnetic storms, consists of the superfountain effect [Tsurutani *et al.*, 2004; Mannucci *et al.*, 2005; Balan *et al.*, 2009, 2011]. We have demonstrated that during moderate storms the equatorial anomaly develops but can have highly asymmetric crests due to the action of a persistent meridional wind. It was also shown that during the storms of August 2010 and 2011, the crests of the anomaly did not move to latitudes poleward of 20°. In fact, in one case the anomaly appears to move equatorward and cross into the opposite hemisphere. Despite the lack of density contributions from equatorial latitudes, prominent SEDs developed during both storms implying that the source of the plasma within the SEDs was confined and localized to midlatitudes. It is concluded that during these two storms no density was transported from low latitudes either to form the SED or to create the second TEC enhancement that was observed in the TEC maps. The confinement of the anomaly to latitudes less than 20° implies the existence of a small penetration electric field during both storms.

Several authors have suggested that subauroral SEDs can be formed by the transport of plasma that originates at equatorial latitudes [Tsurutani *et al.*, 2004; Mannucci *et al.*, 2005]. Other researchers have postulated that plasma from the crests of the anomaly can be transported poleward by the action of prompt penetrating  $E$  fields at midlatitudes [Kelley *et al.*, 2004]. To fully resolve the question on the origin of the SED, it is necessary to contemplate the motion of TEC structures as they are tracers of the plasma dynamics during moderate and superstorms. Here it is suggested that during moderate storms the origin of the plasma within the SEDs is in the region adjacent to the TEC enhancements and driven to higher altitudes by the wind system and electric fields [Heelis *et al.*, 2009; Rishbeth *et al.*, 2010]. Our contention is supported by the decrease in ion temperature that is simultaneously measured by the DMSP satellites when crossing the SED and the second TEC enhancement.

The SSIES instrument on board the DMSP-F15 and F17 satellites observed several events of ion temperature decrease when the satellites passed close to the region of enhanced TEC values. These measurements have some similarities to early satellite observations conducted at low latitudes by Hanson *et al.* [1970, 1973], Hanson and Sanatani [1970], and Heelis *et al.* [1978] in which the ion temperature above 500 km was less than the neutral temperature. These authors and also Venkatraman and Heelis [1999] suggested that the low-latitude plasma had been adiabatically cooled owing to the upward expansion of plasma during interhemispheric transport along magnetic field lines. For a flow from summer to winter, the ion temperature was lowered on the summer side and raised on the winter side. Bailey *et al.* [1973] and Bailey and Heelis [1980] solved the heat balance equation together with the momentum equation for  $O^+$ ,  $H^+$ , and electrons to demonstrate that ion temperature troughs depend on the neutral wind velocity and thermal conduction. Satellite measurements during solar minimum conditions have indicated that  $T_i$  cooling and heating are strongly dependent on the location of the  $O^+/H^+$  transition height. During solar maximum conditions the transition height is well above 800 km. During solar minimum conditions the transition height lowers in altitude, and the cooling process is not as strong as during high solar activity [Venkatraman and Heelis, 1999]. We observed a smaller amount of cooling in 2010 than in 2011, a year of less solar activity. It is suggested that a strong southward directed meridional wind likely associated with the disturbance dynamo is able to move plasma up the field lines and produce the second TEC enhancement and influence the altitudinal distribution of the SED. During both storms the plasma moves up the magnetic field, inducing an adiabatic plasma cooling.

During geomagnetic storms, significant changes in the neutral composition are typically observed [Lei *et al.*, 2008; Crowley *et al.*, 2008]. This composition variability has been evident in the  $O/N_2$  ratio measured by the Global Ultraviolet Imager on the Thermosphere Ionosphere Mesosphere Energetics and Dynamics satellite. An increase in the  $O/N_2$  ratio can certainly produce an increase in the local density and the altitude-integrated TEC values. However, these density enhancements will not be associated with adiabatic expansions or compressions of the plasma. Therefore, no variability in the ion temperature would be expected.

The storms of August 2010 and 2011 have also shown unique characteristics not reported before. The maps of Figures 2 and 5 display two regions, both at midlatitudes, containing enhanced TEC values. We believe that the appearance of a second region of enhanced TEC over Central America is mainly produced by the seasonal variability of the density at midlatitudes, the meridional wind system, and the peculiar geometry of the magnetic field in the American sector that contains a negative declination at longitudes west of 70°W. The high magnetic declination of the Earth's magnetic field in the Central American sector allows a westward

zonal wind to move plasma up the field lines [Zhang *et al.*, 2011, 2012; Valladares, 2013]. The westward zonal wind and a meridional wind directed southward, likely associated with the storm disturbance dynamo, can initiate a transport of the local plasma along and up the field lines, consequently slowing the plasma recombination rate. We also observed the merging of the second region of enhanced TEC and the southern part of the SED. The merging of both TEC enhanced regions occurred at 23:10 UT on 3 August 2010 (Figure 2c) and at 23:00 UT on 5 August 2011 (Figure 5c). The final fate of these two TEC-enhanced regions also shows quite similar characteristics. During the storms of August 2010 and August 2011, the merged regions separate and decay independently after 01:00 UT.

It is also indicated that if the  $B_z$  southward turning would have occurred at a different time, especially when the density is low, say between midnight and sunset, then probably no second TEC enhancement would have occurred due to the absence of sufficient plasma to be transported along the field lines. Moreover, both storms occurred during Northern Hemisphere summer solstice when the ionospheric plasma is larger in northern latitudes.

The formation of SEDs has been associated with subauroral polarization streams (SAPS). SAPS is a broad and poleward directed electric field which drives sunward plasma convection at subauroral latitudes in the evening local time sector [Foster and Burke, 2002]. SAPS also produce erosion of the dusk-sector plasmasphere and the formation of sunward directed plasmasphere drainage plumes.

Prominent TEC troughs developed poleward and a few hours after the initiation of the SED during both storms. However, the in situ DMSP data indicated the presence of plasma troughs as early as 21:34 UT on 3 August 2010 and 22:28 UT on 5 August 2011. This is few hours before they were imaged using GPS TEC observations.

It is worth pointing out that the much larger number of GPS receivers that are presently operating in South and Central America and the Caribbean region allowed us to have the necessary spatial resolution to understand the dynamics of the processes creating the TEC enhancements.

## 5. Conclusions

We have used maps of TEC over the American sector to investigate the spatial extent and temporal evolution of TEC enhancements during two moderate storms that developed on August 2010 and 2011. In addition to the equatorial anomaly, there exist two regions containing enhanced TEC values at midlatitudes: the SED and another region called here the second TEC enhancement. Although SEDs have been observed during all seasons, the appearance of the second TEC enhancements seems restricted to Northern Hemisphere summer conditions.

We have shown that during two moderate storms the plasma density within the SEDs does not originate from the equatorial anomaly as the anomaly crests do not move poleward of 20° magnetic latitude. It is also indicated that the TEC along the SED forms all at once and is not transported from farther eastward locations. More observations are necessary to assess SED formation during other seasons. The appearance and evolution of the SED is consistent with the plasma dynamics described by Heelis *et al.* [2009] in which local plasma moves to higher altitudes due to a zonal  $E$  field. However, it is indicated that a southward directed neutral wind acting across the North American continent could also help plasma reach higher altitudes. During both storms the SEDs are observed to move equatorward and are associated with an equatorward expansion of the auroral oval.

A second region containing enhanced TEC at midlatitudes was observed during both storms. We believe that these enhancements are the response of  $F$  region densities to neutral winds that push plasma up the field lines to altitudes where recombination proceeds at a slower pace. The second region of enhanced TEC merges with the SED in both storms developing finger-type structures that appear to be associated with a large-scale plasma instability.

## References

- Bailey, G. J., and R. A. Heelis (1980), Ion temperature troughs induced by a meridional neutral air wind in the night-time equatorial topside ionosphere, *Planet. Space Sci.*, *28*, 895–906, doi:10.1016/0032-0633(80)90062-8.
- Bailey, G. J., R. J. Moffett, W. B. Hanson, and S. Sanatani (1973), Effects of interhemisphere transport on plasma temperatures at low latitudes, *J. Geophys. Res.*, *78*, 5597–5610, doi:10.1029/JA078i025p05597.
- Balan, N., K. Shiokawa, Y. Otsuka, S. Watanabe, and G. J. Bailey (2009), Super plasma fountain and equatorial ionization anomaly during penetration electric field, *J. Geophys. Res.*, *114*, A03310, doi:10.1029/2008JA013768.

### Acknowledgments

The authors would like to thank Claudio Brunini and Mauricio Gende of the Geocentric Reference System for the Americas (SIRGAS) and Michael Bevis from Ohio State University-Central and Southern Andes GPS Project (OSU-CAP) for providing GPS data that were used in this study. Hector Mora from the Colombian Institute of Geology and Mining (INGEOMINAS) provided RINEX files from several stations in Colombia. His help is greatly appreciated. One of the authors, Valladares, was partially supported by NSF grants ATM-1242476 and ATM-1135675. The Low Latitude Ionospheric Sensor Network (LISN) is a project led by Boston College in collaboration with the Geophysical Institute of Perú and other institutions that provide information in benefit of the scientific community. J.M.R. acknowledges the support of NSF under award AGS-1242038. We thank all organizations and persons that are supporting and operating receivers in LISN. The TEC values presented in this publication are stored in the LISN web page (<http://lisn.igp.gob.pe>).

- Balan, N., K. Shiokawa, Y. Otsuka, T. Kikuchi, D. Vijaya Lekshmi, S. Kawamura, M. Yamamoto, and G. J. Bailey (2010), A physical mechanism of positive ionospheric storms at low latitudes and midlatitudes, *J. Geophys. Res.*, *115*, A02304, doi:10.1029/2009JA014515.
- Balan, N., et al. (2011), A statistical study of the response of the dayside equatorial  $F_2$  layer to the main phase of intense geomagnetic storms as an indicator of penetration electric field, *J. Geophys. Res.*, *116*, A03323, doi:10.1029/2010JA016001.
- Basu, S., S. Basu, K. M. Groves, H.-C. Yeh, S.-Y. Su, F. J. Rich, P. J. Sultan, and M. J. Keskinen (2001), Response of the equatorial ionosphere in the South Atlantic Region to the great magnetic storm of July 15, 2000, *Geophys. Res. Lett.*, *28*, 3577–3580, doi:10.1029/2001GL013259.
- Basu, S., S. Basu, F. J. Rich, K. M. Groves, E. MacKenzie, C. Coker, Y. Sahai, P. R. Fagundes, and F. Becker-Guedes (2007), Response of the equatorial ionosphere to prompt penetration electric fields during intense magnetic storms, *J. Geophys. Res.*, *112*, A08308, doi:10.1029/2006JA012192.
- Crowley, G., et al. (2006), Global thermosphere-ionosphere response to onset of 20 November 2003 magnetic storm, *J. Geophys. Res.*, *111*, A10518, doi:10.1029/2005JA011518.
- Crowley, G., A. Reynolds, J. P. Thayer, J. Lei, L. J. Paxton, A. B. Christensen, Y. Zhang, R. R. Meier, and D. J. Strickland (2008), Periodic modulations in thermospheric composition by solar wind high speed streams, *Geophys. Res. Lett.*, *35*, L21106, doi:10.1029/2008GL035745.
- Foster, J. C. (1993), Storm time plasma transport at middle and high latitudes, *J. Geophys. Res.*, *98*, 1675–1689, doi:10.1029/92JA02032.
- Foster, J. C., and A. J. Coster (2007), Conjugate localized enhancement of total electron content at low latitudes in the American sector, *J. Atmos. Sol. Terr. Phys.*, *69*(10–11), 1241–1252, doi:10.1016/j.jastp.2006.09.012.
- Foster, J. C., and F. J. Rich (1998), Prompt mid-latitude electric field effects during severe geomagnetic storms, *J. Geophys. Res.*, *103*, 26,367–26,372, doi:10.1029/97JA03057.
- Foster, J. C., and W. J. Burke (2002), SAPS: A new categorization for sub-auroral electric fields, *Eos Trans. AGU*, *83*, 393–394, doi:10.1029/2002EO000289.
- Foster, J. C., et al. (2005), Multiradar observations of the polar tongue of ionization, *J. Geophys. Res.*, *110*, A09S31, doi:10.1029/2004JA010928.
- Hanson, W. B., and S. Sanatani (1970), Meteoric ions above the  $F_2$  peak, *J. Geophys. Res.*, *75*, 5503–5509, doi:10.1029/JA075i028p05503.
- Hanson, W. B., S. Sanatani, D. Zuccaro, and T. W. Flowerday (1970), Plasma measurements with the retarding potential analyzer on OGO 6, *J. Geophys. Res.*, *75*, 5483–5501, doi:10.1029/JA075i028p05483.
- Hanson, W. B., A. F. Nagy, and R. J. Moffett (1973), OGO 6 measurements of supercooled plasma in the equatorial exosphere, *J. Geophys. Res.*, *78*, 751, doi:10.1029/JA078i004p00751.
- Heelis, R. A., and S. Mohapatra (2009), Storm time signatures of the ionospheric zonal ion drift at middle latitudes, *J. Geophys. Res.*, *114*, A02305, doi:10.1029/2008JA013620.
- Heelis, R. A., G. J. Bailey, and W. B. Hanson (1978), Ion temperature troughs and interhemispheric transport observed in the equatorial ionosphere, *J. Geophys. Res.*, *83*, 3683–3689, doi:10.1029/JA083iA08p03683.
- Heelis, R. A., J. J. Sojka, M. David, and R. W. Schunk (2009), Storm time density enhancements in the middle-latitude dayside ionosphere, *J. Geophys. Res.*, *114*, A03315, doi:10.1029/2008JA013690.
- Kelley, M. C., M. N. Vlasov, J. C. Foster, and A. J. Coster (2004), A quantitative explanation for the phenomenon known as storm-enhanced density, *Geophys. Res. Lett.*, *31*, L19809, doi:10.1029/2004GL020875.
- Lei, J., J. P. Thayer, J. M. Forbes, E. K. Sutton, and R. S. Nerem (2008), Rotating solar coronal holes and periodic modulation of the upper atmosphere, *Geophys. Res. Lett.*, *35*, L10109, doi:10.1029/2008GL033875.
- Mannucci, A. J., B. T. Tsurutani, B. A. Iijima, A. Komjathy, A. Saito, W. D. Gonzalez, F. L. Guarnieri, J. U. Kozyra, and R. Skoug (2005), Dayside global ionospheric response to the major interplanetary events of October 29–30, 2003 “Halloween Storms”, *Geophys. Res. Lett.*, *32*, L12502, doi:10.1029/2004GL021467.
- Perkins, F. (1973), Spread  $F$  and ionospheric currents, *J. Geophys. Res.*, *78*, 218–226, doi:10.1029/JA078i001p00218.
- Rishbeth, H., R. A. Heelis, J. J. Makela, and S. Basu (2010), Storming the Bastille: the effect of electric fields on the ionospheric  $F$ -layer, *Ann. Geophys.*, *28*, 977, doi:10.5194/angeo-28-977-2010.
- Schunk, R. W. (1988), A mathematical model of middle and high-latitude ionosphere, *PAGEOPH*, *127*, 255–303, doi:10.1007/BF00879813.
- Schunk, R. W., J. J. Sojka, and M. D. Bowline (1986), Theoretical study of the electron temperature in the high-latitude ionosphere for solar maximum and winter conditions, *J. Geophys. Res.*, *91*, 12,041, doi:10.1029/JA091iA11p12041.
- Sojka, J. J. (1989), Global scale, physical models of the  $F$  region ionosphere, *Rev. Geophys.*, *27*, 371–403, doi:10.1029/RG027i003p00371.
- Tsurutani, B. T., et al. (2004), Global dayside ionospheric uplift and enhancement associated with interplanetary electric fields, *J. Geophys. Res.*, *109*, A08302, doi:10.1029/2003JA010342.
- Tsurutani, B. T., A. J. Mannucci, O. P. Verkhoglyadova, and G. S. Lakhina (2013), Comment on “Storming the Bastille: the effect of electric fields on the ionospheric  $F$ -layer” by Rishbeth et al. (2010), *Ann. Geophys.*, *31*, 145–150, doi:10.5194/angeo-31-145-2013.
- Valladares, C. E. (2013), LISN: Measurement of TEC values, and TID characteristics over South and Central America, Abstract SA12A-06 presented at 2013 Fall Meeting, AGU, San Francisco, Calif., 9–13 Dec.
- Valladares, C. E., and J. L. Chau (2012), The low-latitude ionosphere sensor network: Initial results, *Radio Sci.*, *47*, RS0L17, doi:10.1029/2011RS004978.
- Venkatraman, S., and R. Heelis (1999), Effects of solar activity variations on adiabatic heating and cooling effects in the nighttime equatorial topside ionosphere, *J. Geophys. Res.*, *104*, 17,117–17,126, doi:10.1029/1999JA00196.
- Vlasov, M., M. C. Kelley, and H. Kil (2003), Analysis of ground-based and satellite observations of  $F$ -region behavior during the great storm of July 15, 2000, *J. Atmos. Sol. Terr. Phys.*, *65*, 1123–1234, doi:10.1016/j.jastp.2003.08.012.
- Zhang, S.-R., J. C. Foster, A. J. Coster, and P. J. Erickson (2011), East-West Coast differences in total electron content over the continental US, *Geophys. Res. Lett.*, *38*, L19101, doi:10.1029/2011GL049116.
- Zhang, S.-R., J. C. Foster, J. M. Holt, P. J. Erickson, and A. J. Coster (2012), Magnetic declination and zonal wind effects on longitudinal differences of ionospheric electron density at midlatitudes, *J. Geophys. Res.*, *117*, A08329, doi:10.1029/2012JA017954.